Force-Induced Near-Infrared Chromism of Mechanophore-Linked Polymers

Journal:	*Journal of the American Chemical Society*
Manuscript ID	ja-2021-05923k
Manuscript Type:	Communication
Date Submitted by the Author:	08-Jun-2021
Complete List of Authors:	Qi, Qingkai; Clarkson University, Sekhon, Gaganjot; Clarkson University, Department of Chemical & Biomolecular Engineering Chandradat, Richard; Clarkson University Department of Chemistry and Biomolecular Science Ofodum, Nnamdi; Clarkson University Department of Chemistry and Biomolecular Science Shen, Tianruo; Singapore University of Technology and Design Scrimgeour, Jan; Clarkson University, Department of Physics Joy, Monu; Clarkson University, Department of Chemistry & Biomolecular Science Wriedt, Mario; Clarkson University, Department of Chemistry & Biomolecular Science Jayathirtha, Madhuri; Clarkson University Department of Chemistry and Biomolecular Science Darie, Costel; Clarkson University, Chemistry & Biomolecular Science Shipp, Devon; Clarkson University, Department of Chemistry Liu, Xiaogang; Singapore University of Technology and Design, Science and Math Cluster Lu, Xiaocun; Clarkson University Department of Chemistry and Biomolecular Science,

Force-Induced Near-Infrared Chromism of Mechanophore-Linked Polymers

Qingkai Qi,† Gaganjot Sekhon,# Richard Chandradat,† Nnamdi M. Ofodum,† Tianruo Shen,‡ Jan Scrimgeour,⊥ Monu Joy,† Mario Wriedt,† Madhuri Jayathirtha,† Costel C. Darie,† Devon A. Shipp,† Xiaogang Liu,*‡ and Xiaocun Lu*†

†Department of Chemistry & Biomolecular Science, ⊥Department of Physics, #Department of Chemical & Biomolecular Engineering, Clarkson University, 8 Clarkson Ave, Potsdam, New York 13699, United States.

‡Fluorescence Research Group, Singapore University of Technology and Design, 8 Somapah Road, Singapore 487372, Singapore.

ABSTRACT: A near-infrared (NIR) mechanophore was developed and incorporated into a poly(methyl acrylate) chain to showcase the first force-induced NIR chromism in polymeric materials. This mechanophore, based on benzo[1,3]oxazine (OX) fused with a heptamethine cyanine moiety, exhibited NIR mechanochromism in solution, thin-film, and bulk states. The mechanochemical activity was validated using UV-vis-NIR absorption/fluorescence spectroscopies, gel permeation chromatography (GPC), NMR, and DFT simulations. Our work demonstrates that NIR mechanochromic polymers have considerable potential in mechanical force sensing, force mapping, biological imaging, and biomechanics.

Polymer mechanochemistry[1] endows a unique method for triggering selective chemical transformations in which mechanical force inputs are converted to various outputs, including color and fluorescent variation,[2] chemiluminescence,[3] small molecule[4] and drug release,[5] catalyst generation,[6] and reaction pathway alteration.[7] In the past decade, research into polymer mechanochemistry has made substantial progress in single-molecule force spectroscopy,[8] mechanochemical degradation of polymers,[9] cascade unzipping of ladderanes,[10] regioisomeric mechanoreactivity,[11] mechanochemistry of supramolecular architectures,[12] and mechano-activation in biological systems.[13] In particular, mechanophore-based chromism has demonstrated significant advantages in force mapping and *in-situ* mechanics sensing in a wide range of polymeric materials.[14]

Several classes of mechanochromic mechanophores have been reported, such as spiropyran,[2b, 15] naphthopyran,[2b, 11b] rhodamine,[16] Diels-Alder adducts,[17] and radical systems.[18] Due to limited π-conjugation sizes, these mechanophores demonstrated mechanically activated visible color (absorption) or fluorescence (emission) changes only in the UV-vis region. However, near-infrared (NIR) luminescence is more favorable in bioimaging,[19] medical diagnostics,[20] anti-counterfeiting,[21] and optical storage[22] owing to their deep penetration depth, low background noise (i.e., by avoiding autofluorescence), and low phototoxicity.[23] Developing NIR mechanophores could, therefore, greatly expand the applications of mechanochemistry. Unfortunately, expanding the π-conjugation of mechanophores toward the NIR luminescence poses synthetic challenges and affects molecular packing and efficacy of mechanical responses, creating a significant yet unexplored challenge.

This paper reports the first near-infrared mechanophore with a fused oxazine-heptamethine cyanine (OHC) structure to showcase mechanochemically-induced NIR chromism in polymeric materials (Scheme 1). We demonstrate that this NIR mechanophore could be mechanically activated in solution (*via* ultrasonication), thin-film (*via* blade-cutting), and bulk state in a polymer matrix (*via* impact), endowing it with considerable potential in various applications, such as molecular logic gates and force sensing.

Scheme 1. Molecular design strategy of the near-infrared mechanophore OHC.

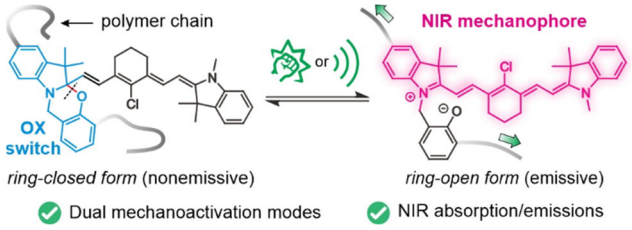

The structural design of the OHC mechanophore combines a benzo[1,3]oxazine-based mechanical switch (OX) and a classic NIR heptamethine cyanine (HC) fluorophore (Scheme 1). HC is highly fluorescent in the cationic form due to its extended conjugation and charge delocalization; however, it becomes non-emissive in its neutral form.[24] The mechanical switch OX, according to the latest research from our group and a recent literature report,[11c] represents an efficient mechanophore with rapid dynamics, versatile functionalization, and diverse regioisomeric mechanosensitive modes. We reasoned that introducing an OX

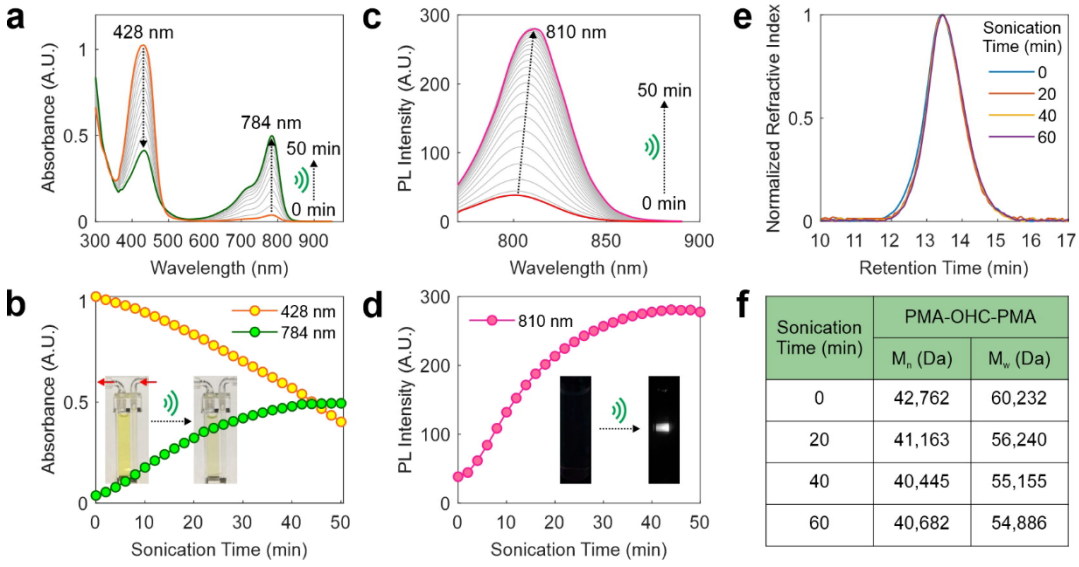

f

Sonication Time (min)	PMA-OHC-PMA	
	M_n (Da)	M_w (Da)
0	42,762	60,232
20	41,163	56,240
40	40,445	55,155
60	40,682	54,886

Figure 1. (a) UV-vis-NIR absorption spectra and (b) corresponding kinetics, (c) Photoluminescence (PL) spectra and (d) corresponding kinetics of PMA-OHC-PMA (1.5 mg/mL in CH_3CN) under ultrasonication; Insets of (b) and (d): Visual and fluorescent images of the solution before and after ultrasonication. (e) Time-dependent GPC traces and (f) the number-average molecular weight (M_n) and the weight-average molecular weight (M_w) of PMA-OHC-PMA under ultrasonication.

cage to cap the HC nitrogen *via* a covalent C-O bond might modulate the charge state of cyanine, resulting in a structural switch between a ring-closed form (CF; non-emissive) and a ring-open form (OF; emissive). Accordingly, the mechanically triggered ring-opening of OX could modify the cyanine conjugation length and thereby control the optical properties of the HC moiety, enabling a near-infrared mechanophore OHC.

Motivated by this design strategy, we synthesized a dibromoisobutyryl-functionalized OHC initiator Br-OHC-Br, followed by an atom transfer radical polymerization (ATRP) to incorporate the OHC mechanophore into the center of a poly(methyl acrylate) (PMA) chain (Supporting Information). The OHC-centered PMA chain allows us to test the mechanochemical reactivity of OHC both in solution and bulk states under various mechanical force modes, including ultrasonication, scratching, and impact.

The ring-opening behavior of OHC was first studied in solution by UV-vis-NIR absorption and ^{1}H NMR spectroscopy. Oxazine exhibits reversible switching between its OF and CF states tuned by acid-base stimuli.[25] Such switching is reflected by significant changes in UV-vis-NIR absorption maxima at 430 nm and 781 nm in Br-OHC-Br (assigned to the CF and OF states, respectively, owing to their different π-conjugation sizes as well as the characteristic NIR absorption band of the cationic HC unit, Figure S1). These assignments were confirmed by using ^{1}H NMR spectroscopy. The methylene hydrogens and alkenyl hydrogens adjacent to the indoline unit showed significant downfield shifts in the OF state because of the positively charged indoline nitrogen (Figure S2). Upon treating the OF state with a base, the equilibrium shifted to the neutral CF state, with proton signals ultimately returning to their ring-closed positions.

We next tested and confirmed the mechanochemical reactivity of PMA-OHC-PMA in the solution state using ultrasonication. Ultrasonication is a well-established method to test mechanophore reactivity in solution by taking advantage of dynamic acoustic cavitation to generate polymer chain pulling, followed by applying a molecular stretching force to the chain-centered mechanophore.[26] Pulsed ultrasonication (1s on and 1s off) was applied to a dilute acetonitrile solution of PMA-OHC-PMA (1.5 mg/mL) for 50 min. A flow cell cuvette was hooked up to the sonication cell to collect real-time UV-vis-NIR absorption data.

The mechanophore reactivity of PMA-OHC-PMA in solution was confirmed using UV-vis-NIR absorption/fluorescence spectroscopies and gel permeation chromatography (GPC) (Figure 1). As predicted in our mechanophore design, a NIR absorption band peaked at 784 nm (due to the OF state) gradually enhanced during the ultrasonication (Figure 1a,b). Concurrently, the UV-vis absorption band peaked at 428 nm (due to the CF state) progressively decreased. The UV-vis-NIR absorption spectra of the ultrasonication treated PMA-OHC-PMA and the acid-induced OF state of Br-OHC-Br showed a negligible difference, confirming that mechanical force generated by ultrasonication led to the ring-opening of the OHC mechanophore in acetonitrile. As expected, the OF state of PMA-OHC-PMA is fluorescent, with an emission peak at ~810 nm (Figure 1c,d). Based on our exponential fitting to the emission intensity as a function of time, the ultrasonication-induced NIR emission showed a reaction rate of 0.071 min^{-1} (Figure S3). Detailed photophysical parameters of PMA-OHC-PMA under ultrasonication were summarized in Table 1. The molecular weight of PMA-OHC-PMA was also monitored by GPC during 60-min ultrasonication. No significant molecular weight changes were detected (Figure 1e,f), suggesting that no chain scission occurred during the ultrasonication.

Table 1. Summary of photophysical parameters of PMA-OHC-PMA under ultrasonication.

ε_{CF} (M^{-1} cm^{-1})[a]	ε_{OF} ($M^{-1}cm^{-1}$)[a]	$\lambda_{abs,\,CF}$ (nm)[b]	A_{CF}[b]	$\lambda_{abs,\,OF}$ (nm)[b]	A_{OF}[b]	$\lambda_{em,\,OF}$ (nm)[c]	$\Phi_{CF\rightarrow OF}$ (%)[d]
49,835	138,842	428	1.02	784	0.5	812	26.4

[a]Molar extinction coefficients (ε_{CF} and ε_{OF}) of UV-vis-NIR absorption peaks of the CF and OF states of Br-OHC-Br (10^{-5} M in acetonitrile); the OF state was obtained by pre-addition of trifluoroacetic acid (TFA, 0.1% v/v) to the sample solution; [b]Peak UV-vis-NIR absorption wavelengths ($\lambda_{abs,\,CF}$ and $\lambda_{abs,\,OF}$) and corresponding absorbances (A_{CF} and A_{OF}), and [c]peak PL emission wavelength ($\lambda_{em,\,OF}$) of PMA-OHC-PMA (1.5 mg/mL in acetonitrile) before and after sonication (50 min); [d]$\Phi_{CF\rightarrow OF}$ (%) = C_{OF}/C_{total} ×100%, was the sonication-induced ring-opening reaction yield.

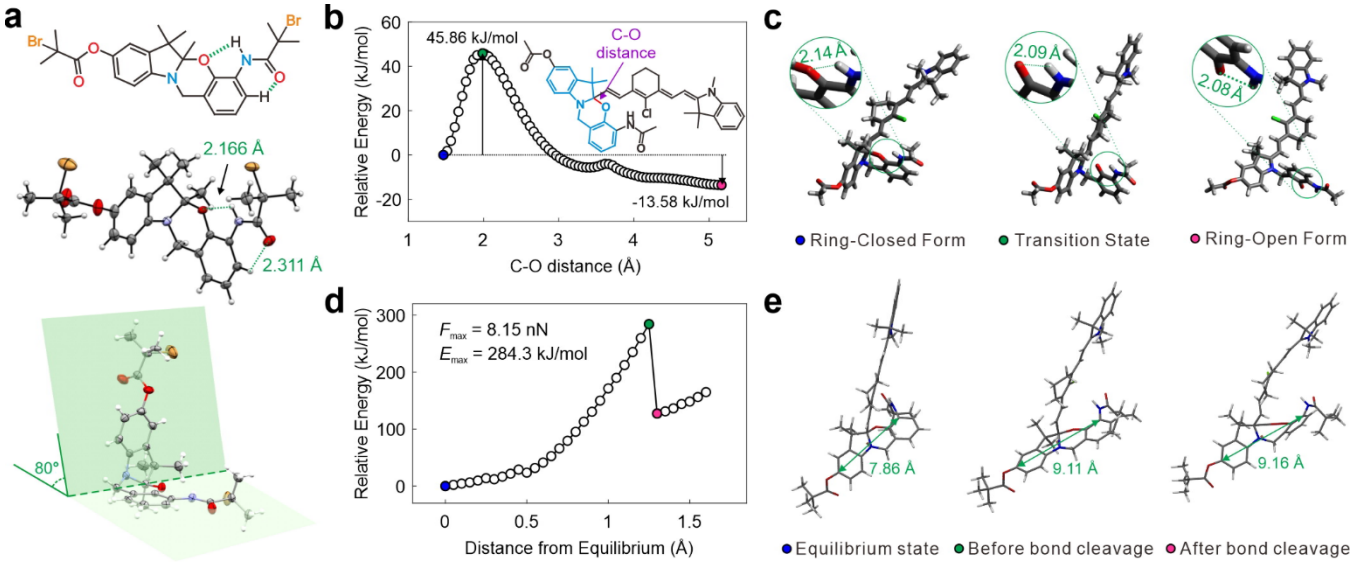

Figure 2. (a) ORTEP drawings (50% probability ellipsoids) with selected intramolecular H-bonding and dihedral angle in the single crystal of Br-OX-Br; (b) Potential energy surface of simplified OHC as a function of the C-O distance in acetonitrile; (c) Optimized geometries of simplified OHC in the ring-closed form, at the transition state, and in the ring-open form in acetonitrile; (d) Potential energy surface of OHC plotted as a function of displacement from equilibrium. The inset shows E_{max} (the bond dissociation energy) and F_{max} (the maximum force) immediately before bond rupture; (e) Optimized structures at critical points in the CoGEF calculations.

To further validate the mechanochemical reactivity of the OHC mechanophore, two control compounds, Br-OHC-Br (OHC with no PMA chain attached, Scheme S1) and OHC-PMA (OHC at the PMA chain end, Scheme S2), were tested under identical ultrasonication conditions. Neither control compound was susceptible to ultrasonication-induced mechanical force because mechanophores located in the center of the polymer chain were more readily activated, owing to efficient stretching by the two polymer sidechains.[26] Indeed, no NIR absorption band was observed during 60-min ultrasonication for the small molecule Br-OHC-Br (Figure S4a). Similarly, ultrasonication of the OHC-PMA solution showed a very weak absorption band at 784 nm (Figure S4b), suggesting that only a small fraction of OHC-PMA was mechanically activated.

The same contrast in the mechanochemical activity was also observed in the solid state, where OHC-PMA remained inactive (Figure S5) but PMA-OHC-PMA was responsive to impact (see more details later). These control experiments collectively validated that OHC was only activated by mechanical force.

The single-crystal structure of an OHC derivative, Br-OX-Br, was obtained and formed a foundation to establish a clear correlation between the mechanosensitivity and molecular structures (Figures 2a and S6; Table S1). Br-OX-Br showed a nearly perpendicular configuration between the benzoxazine plane and the indoline plane with an 80° dihedral angle (Figure 2a). The C-O bond cleaved by mechanical force was located close to the intersection of the benzoxazine-indoline planes. In the crystal structure, two intramolecular hydrogen bonds were detected at the amide group, with bonding distances for C-O···H-N and C=O···H-C of 2.166 Å and 2.311 Å, respectively.

Based on this crystal structure, we built and optimized the three-dimensional geometries of OHC and scanned its potential energy surface along with the breakage of the C-O bond in the ground state in acetonitrile (Figure 2b). This bond breakage was accompanied by the bending of benzoxazine-indoline planes and the flattering of the HC scaffold, with an energy barrier of 45.86 kJ·mol^{-1}. Our calculations also showed that the OF state of OHC was more stable than the CF state by 13.58 kJ·mol^{-1}. The DFT-derived intramolecular hydrogen-bonding distance of OHC (2.14 Å) matched very well to that of the crystal structure (2.166 Å; Figure 2c) in the CF state, corroborating the accuracy of our calculations. Moreover, DFT calculations showed that this H-bonding distance became even shorter (2.08 Å) in the OF state. These results revealed that the intramolecular hydrogen bonding facilitated the mechanochemical activation of OHC.

The CoGEF (Constrained Geometries simulate External Force) simulation[27] also validated the mechanochemical

activity of the OHC mechanophore. This DFT-based simulation scanned the distance between two designated atoms *via* a stepwise increment to simulate mechanical stretching applied to these two atoms. Figure 2d showed a plot of the increased energy *vs.* the distance increment throughout the molecule elongation. After reaching an energy maximum of 284.3 kJ·mol^{-1}, the C-O bond was cleaved (Figure 2e), leading to a subsequent sharp energy decrease. The maximum force was calculated to be 8.15 nN based on the tangent slope right before the rupture point.

Finally, we explored potential applications of the OHC mechanophore based on its versatile mechanical sensitivity in both solution and solid states. Molecular logic gates have attracted considerable research interests in understanding life sciences and complementing silicon-based computing.[28] Nevertheless, most molecular logic gates use chemical inputs, requiring direct contact and creating substantial complexities concerning precise spatial and temporal control. In contrast, the fluorescent output of the OHC mechanophore could be controlled by two clean, instantaneous, and precise physical inputs—ultrasonication and NIR excitation-light—in a non-contact way. The presence of these two inputs could light up a star-shaped object filled with a PMA-OHC-PMA solution, acting as an "AND" gate with its unique truth table (Figure 3a).

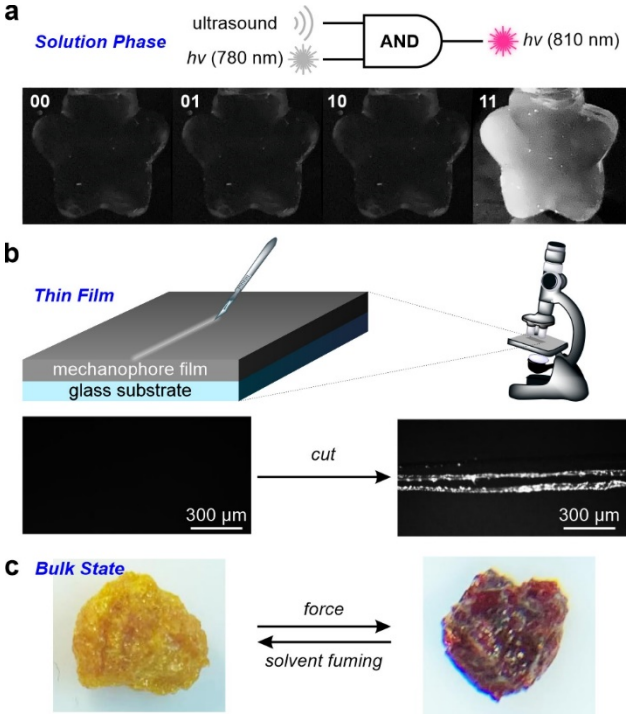

Figure 3. (a) An PMA-OHC-PMA based "AND" gate, with both NIR excitation-light and ultrasonication as inputs. 0 and 1 refer to input states of the truth table. (b) Schematic illustration of a blade-cut PMA-OHC-PMA film and its fluorescence image under microscopy. (c) The reversible color change of the OHC-centered PMA tuned by mechanical force and solvation in the bulk state.

Moreover, PMA-OHC-PMA was mechanochemically activated in both thin-film and bulk states. Under fluorescence microscopy equipped with a NIR-sensitive EMCCD, bright NIR emission was detected only in a blade-cut area under a 660 nm LED illumination (Figure 3b). The bulk PMA-OHC-PMA sample was also mechanically activated by impact (Figure 3c). Notably, the OF state of PMA-OHC-PMA in the bulk state was dark red. Upon dissolution in various aprotic solvents, the red color immediately disappeared. After solvent evaporation, the PMA-OHC-PMA bulk samples became yellowish and ready for mechanical activation again.

In summary, we reported the first near-infrared mechanophore, OHC, by installing a mechanically activatable oxazine cage to a heptamethine cyanine motif. When the OHC mechanophore was introduced to the center of a PMA chain, PMA-OHC-PMA was mechanochemically responsive in solution, thin-film, and bulk states. The mechanochemical activation of OHC was confirmed and validated by UV-vis-NIR absorption/emission, NMR, GPC, and DFT/CoGEF simulations. We anticipate that the OHC mechanophore will inspire the design of a series of NIR mechanophores with tunable NIR wavelengths, including the NIR-II regime. With structural optimizations for water-compatible environments, the OHC mechanophore will open new avenues toward various promising applications in bioimaging and biomechanics.

ASSOCIATED CONTENT

Supporting Information

The Supporting Information is available free of charge on the ACS Publications website. General methods, experiment procedures, computational methods, and characterization (NMR, GPC, and single-crystal data) are included.

AUTHOR INFORMATION

Corresponding Author

* xlu@clarkson.edu; xiaogang_liu@sutd.edu.sg

ACKNOWLEDGMENT

This work was supported by a start-up fund provided by Clarkson University (X.Lu), A*STAR under its AME Program (A2083c0051, X.Liu), the Ministry of Education, Singapore (MOE-MOET2EP10120-0007, X.Liu), and a National Science Foundation award (DMR 1847786, J.S.).

REFERENCES

(1) Li, J.; Nagamani, C.; Moore, J. S. Polymer Mechanochemistry: From Destructive to Productive. *Acc. Chem. Res.* **2015,** *48*, 2181-2190.

(2) (a) McFadden, M. E.; Robb, M. J. Force-Dependent Multicolor Mechanochromism from a Single Mechanophore. *J. Am. Chem. Soc.* **2019,** *141*, 11388-11392; (b) Davis, D. A.; Hamilton, A.; Yang, J.; Cremar, L. D.; Van Gough, D.; Potisek, S. L.; Ong, M. T.; Braun, P. V.; Martinez, T. J.; White, S. R.; Moore, J. S.; Sottos, N. R. Force-Induced Activation of Covalent Bonds in Mechanoresponsive Polymeric Materials. *Nature* **2009,** *459*, 68-72; (c) Pan, Y.; Zhang, H.; Xu, P.; Tian, Y.; Wang, C.; Xiang, S.; Boulatov, R.; Weng, W. A Mechanochemical Reaction Cascade for Controlling Load-Strengthening of a Mechanochromic Polymer. *Angew. Chem. Int. Ed.* **2020,** *59*, 21980-21985; (d) Sagara, Y.; Traeger, H.; Li, J.; Okado, Y.; Schrettl, S.; Tamaoki, N.; Weder, C. Mechanically Responsive Luminescent Polymers Based on Supramolecular Cyclophane Mechanophores. *J. Am. Chem. Soc.* **2021,** *143*, 5519-5525.

(3) Chen, Y.; Spiering, A. J. H.; KarthikeyanS; Peters, G. W. M.; Meijer, E. W.; Sijbesma, R. P. Mechanically Induced Chemiluminescence from Polymers Incorporating a 1,2-Dioxetane Unit in the Main Chain. *Nat. Chem.* **2012,** *4*, 559-562.

(4) (a) Hu, X.; Zeng, T.; Husic, C. C.; Robb, M. J. Mechanically Triggered Small Molecule Release from a Masked Furfuryl Carbonate. *J. Am. Chem. Soc.* **2019,** *141*, 15018-15023; (b) Larsen, M. B.; Boydston, A. J. "Flex-Activated" Mechanophores: Using Polymer Mechanochemistry To Direct Bond Bending Activation. *J. Am. Chem. Soc.* **2013,** *135*, 8189-8192; (c) Diesendruck, C. E.; Steinberg, B. D.; Sugai, N.; Silberstein, M. N.; Sottos, N. R.; White, S. R.; Braun, P. V.; Moore, J. S. Proton-Coupled Mechanochemical Transduction: A Mechanogenerated Acid. *J. Am. Chem. Soc.* **2012,** *134*, 12446-12449; (d) Shen, H.; Larsen, M. B.; Roessler, A. G.; Zimmerman, P. M.; Boydston, A. J. Mechanochemical Release of N-Heterocyclic Carbenes from Flex-Activated Mechanophores. *Angew. Chem. Int. Ed.* **2021**, DOI: 10.1002/anie.202100576.

(5) (a) Huo, S.; Zhao, P.; Shi, Z.; Zou, M.; Yang, X.; Warszawik, E.; Loznik, M.; Göstl, R.; Herrmann, A. Mechanochemical bond scission for the activation of drugs. *Nat. Chem.* **2021,** *13*, 131-139; (b) Shi, Z.; Wu, J.; Song, Q.; Göstl, R.; Herrmann, A. Toward Drug Release Using Polymer Mechanochemical Disulfide Scission. *J. Am. Chem. Soc.* **2020,** *142*, 14725-14732.

(6) (a) Michael, P.; Sheidaee Mehr, S. K.; Binder, W. H. Synthesis and characterization of polymer linked copper(I) bis(N-heterocyclic carbene) mechanocatalysts. *J. Polym. Sci., Part A: Polym. Chem.* **2017,** *55*, 3893-3907; (b) Wei, K.; Gao, Z.; Liu, H.; Wu, X.; Wang, F.; Xu, H. Mechanical Activation of Platinum-Acetylide Complex for Olefin Hydrosilylation. *ACS Macro Lett.* **2017,** *6*, 1146-1150; (c) Piermattei, A.; Karthikeyan, S.; Sijbesma, R. P. Activating catalysts with mechanical force. *Nat. Chem.* **2009,** *1*, 133-137; (d) Michael, P.; Binder, W. H. A Mechanochemically Triggered "Click" Catalyst. *Angew. Chem. Int. Ed.* **2015,** *54*, 13918-13922.

(7) (a) Wang, J.; Kouznetsova, T. B.; Craig, S. L. Reactivity and Mechanism of a Mechanically Activated anti-Woodward-Hoffmann-DePuy Reaction. *J. Am. Chem. Soc.* **2015,** *137*, 11554-11557; (b) Wang, J.; Kouznetsova, T. B.; Niu, Z.; Ong, M. T.; Klukovich, H. M.; Rheingold, A. L.; Martinez, T. J.; Craig, S. L. Inducing and quantifying forbidden reactivity with single-molecule polymer mechanochemistry. *Nat. Chem.* **2015,** *7*, 323-327; (c) Lenhardt, J. M.; Ong, M. T.; Choe, R.; Evenhuis, C. R.; Martinez, T. J.; Craig, S. L. Trapping a Diradical Transition State by Mechanochemical Polymer Extension. *Science* **2010,** *329*, 1057-1060; (d) Hickenboth, C. R.; Moore, J. S.; White, S. R.; Sottos, N. R.; Baudry, J.; Wilson, S. R. Biasing reaction pathways with mechanical force. *Nature* **2007,** *446*, 423-427; (e) Stevenson, R.; De Bo, G. Controlling Reactivity by Geometry in Retro-Diels-Alder Reactions under Tension. *J. Am. Chem. Soc.* **2017,** *139*, 16768-16771; (f) Nixon, R.; De Bo, G. Three concomitant C-C dissociation pathways during the mechanical activation of an N-heterocyclic carbene precursor. *Nat. Chem.* **2020,** *12*, 826-831; (g) Brown, C. L.; Bowser, B. H.; Meisner, J.; Kouznetsova, T. B.; Seritan, S.; Martinez, T. J.; Craig, S. L. Substituent Effects in Mechanochemical Allowed and Forbidden Cyclobutene Ring-Opening Reactions. *J. Am. Chem. Soc.* **2021,** *143*, 3846-3855; (h) McFadden, M. E.; Robb, M. J. Generation of an Elusive Permanent Merocyanine via a Unique Mechanochemical Reaction Pathway. *J. Am. Chem. Soc.* **2021**, DOI: 10.1021/jacs.1c03865.

(8) (a) Bowser, B. H.; Wang, S.; Kouznetsova, T. B.; Beech, H. K.; Olsen, B. D.; Rubinstein, M.; Craig, S. L. Single-Event Spectroscopy and Unravelling Kinetics of Covalent Domains Based on Cyclobutane Mechanophores. *J. Am. Chem. Soc.* **2021,** *143*, 5269-5276; (b) Zhang, Y.; Wang, Z.; Kouznetsova, T. B.; Sha, Y.; Xu, E.; Shannahan, L.; Fermen-Coker, M.; Lin, Y.; Tang, C.; Craig, S. L. Distal conformational locks on ferrocene mechanophores guide reaction pathways for increased mechanochemical reactivity. *Nat. Chem.* **2021,** *13*, 56-62; (c) Wang, J.; Kouznetsova, T. B.; Boulatov, R.; Craig, S. L. Mechanical gating of a mechanochemical reaction cascade. *Nat. Commun.* **2016,** *7*, 13433; (d) Zhang, H.; Li, X.; Lin, Y.; Gao, F.; Tang, Z.; Su, P.; Zhang, W.; Xu, Y.; Weng, W.; Boulatov, R. Multimodal mechanophores based on cinnamate dimers. *Nat. Commun.* **2017,** *8*, 1147.

(9) (a) Lin, Y.; Kouznetsova, T. B.; Craig, S. L. Mechanically Gated Degradable Polymers. *J. Am. Chem. Soc.* **2020,** *142*, 2105-2109; (b) Hsu, T.-G.; Zhou, J.; Su, H.-W.; Schrage, B. R.; Ziegler, C. J.; Wang, J. A Polymer with "Locked" Degradability: Superior Backbone Stability and Accessible Degradability Enabled by Mechanophore Installation. *J. Am. Chem. Soc.* **2020,** *142*, 2100-2104.

(10) (a) Yang, J.; Horst, M.; Werby, S. H.; Cegelski, L.; Burns, N. Z.; Xia, Y. Bicyclohexene-peri-naphthalenes: Scalable Synthesis, Diverse Functionalization, Efficient Polymerization, and Facile Mechanoactivation of Their Polymers. *J. Am. Chem. Soc.* **2020,** *142*, 14619-14626; (b) Boswell, B. R.; Mansson, C. M. F.; Cox, J. M.; Jin, Z.; Romaniuk, J. A. H.; Lindquist, K. P.; Cegelski, L.; Xia, Y.; Lopez, S. A.; Burns, N. Z. Mechanochemical synthesis of an elusive fluorinated polyacetylene. *Nat. Chem.* **2021,** *13*, 41-46; (c) Chen, Z.; Zhu, X.; Yang, J.; Mercer, J. A. M.; Burns, N. Z.; Martinez, T. J.; Xia, Y. The cascade unzipping of ladderane reveals dynamic effects in mechanochemistry. *Nat. Chem.* **2020,** *12*, 302-309; (d) Chen, Z.; Mercer, J. A. M.; Zhu, X.; Romaniuk, J. A. H.; Pfattner, R.; Cegelski, L.; Martinez, T. J.; Burns, N. Z.; Xia, Y. Mechanochemical unzipping of insulating polyladderene to semiconducting polyacetylene. *Science* **2017,** *357*, 475-479.

(11) (a) Lin, Y.; Barbee, M. H.; Chang, C.-C.; Craig, S. L. Regiochemical Effects on Mechanophore Activation in Bulk Materials. *J. Am. Chem. Soc.* **2018,** *140*, 15969-15975; (b) Robb, M. J.; Kim, T. A.; Halmes, A. J.; White, S. R.; Sottos, N. R.; Moore, J. S. Regioisomer-Specific Mechanochromism of Naphthopyran in Polymeric Materials. *J. Am. Chem. Soc.* **2016,** *138*, 12328-12331; (c) Qian, H.; Purwanto, N. S.; Ivanoff, D. G.; Halmes, A. J.; Sottos, N. R.; Moore, J. S. Fast, reversible mechanochromism of regioisomeric oxazine mechanophores: Developing in situ responsive force probes for polymeric materials. *Chem* **2021,** *7*, 1080-1091.

(12) (a) De Bo, G. Mechanochemistry of the mechanical bond. *Chem. Sci.* **2018,** *9*, 15-21; (b) Zhang, M.; De Bo, G. A Catenane as a Mechanical Protecting Group. *J. Am. Chem. Soc.* **2020,** *142*, 5029-5033; (c) Shi, C. Y.; Zhang, Q.; Yu, C. Y.; Rao, S. J.; Yang, S.; Tian, H.; Qu, D. H. An Ultrastrong and Highly Stretchable Polyurethane Elastomer Enabled by a Zipper-Like Ring-Sliding Effect. *Adv. Mater.* **2020,** *32*, 2000345; (d) Sagara, Y.; Karman, M.; Seki, A.; Pannipara, M.; Tamaoki, N.; Weder, C. Rotaxane-Based Mechanophores Enable Polymers with Mechanically Switchable White Photoluminescence. *ACS Cent. Sci.* **2019,** *5*, 874-881.

(13) (a) Huang, W.; Wu, X.; Gao, X.; Yu, Y.; Lei, H.; Zhu, Z.; Shi, Y.; Chen, Y.; Qin, M.; Wang, W.; Cao, Y. Maleimide-thiol adducts stabilized through stretching. *Nat. Chem.* **2019,** *11*, 310-319; (b) Zhou, Y.; Huo, S.; Loznik, M.; Göstl, R. Boersma, A. J.; Herrmann, A., Controlling Optical and Catalytic Activity of Genetically Engineered Proteins by Ultrasound. *Angew. Chem. Int. Ed.* **2021,** *60*, 1493-1497; (c) Merindol, R.; Delechiave, G.; Heinen, L.; Catalani, L. H.; Walther, A. Modular Design of Programmable Mechanofluorescent DNA Hydrogels. *Nat. Commun.* **2019,** *10*, 528.

(14) (a) Ducrot, E.; Chen, Y.; Bulters, M.; Sijbesma, R. P.; Creton, C. Toughening Elastomers with Sacrificial Bonds and Watching Them Break. *Science* **2014,** *344*, 186-189; (b) Chen, Y.; Yeh, C. J.; Guo, Q.; Qi, Y.; Long, R.; Creton, C. Fast reversible isomerization of merocyanine as a tool to quantify stress history in elastomers. *Chem. Sci.* **2021,** *12*, 1693-1701; (c) Chen, Y.; Yeh, C. J.; Qi, Y.; Long, R.; Creton, C. From force-responsive molecules to quantifying and mapping stresses in soft materials. *Sci. Adv.* **2020,** *6*, eaaz5093; (d) Baumann, C.; Stratigaki, M.; Centeno, S. P.; Göstl, R. Multicolor Mechanofluorophores for the Quantitative Detection of Covalent Bond Scission in Polymers. *Angew. Chem. Int. Ed.* **2021**, DOI: 10.1002/anie.202101716; (e) Tian, Y.; Cao, X.; Li, X.; Zhang, H.; Sun, C.-L.; Xu, Y.; Weng, W.; Zhang, W.; Boulatov, R. A Polymer with Mechanochemically Active Hidden Length. *J. Am. Chem. Soc.* **2020,** *142*, 18687-18697.

(15) Zhang, H.; Gao, F.; Cao, X.; Li, Y.; Xu, Y.; Weng, W.; Boulatov, R. Mechanochromism and Mechanical-Force-Triggered Cross-Linking from a Single Reactive Moiety Incorporated into Polymer Chains. *Angew. Chem. Int. Ed.* **2016,** *55*, 3040-3044.

(16) (a) Wang, T.; Zhang, N.; Dai, J.; Li, Z.; Bai, W.; Bai, R. Novel Reversible Mechanochromic Elastomer with High Sensitivity: Bond Scission and Bending-Induced Multicolor Switching. *ACS Appl. Mater. Interfaces* **2017,** *9*, 11874-11881; (b) Wu, M.; Guo, Z.; He, W.; Yuan, W.; Chen, Y. Empowering self-reporting polymer blends with orthogonal optical properties responsive in a broader force range. *Chem. Sci.* **2021,** *12*, 1245-1250.

(17) Kabb, C. P.; O'Bryan, C. S.; Morley, C. D.; Angelini, T. E.; Sumerlin, B. S. Anthracene-based mechanophores for compression-activated fluorescence in polymeric networks. *Chem. Sci.* **2019,** *10*, 7702-7708.

(18) (a) Imato, K.; Irie, A.; Kosuge, T.; Ohishi, T.; Nishihara, M.; Takahara, A.; Otsuka, H. Mechanophores with a Reversible Radical System and Freezing-Induced Mechanochemistry in Polymer Solutions and Gels. *Angew. Chem. Int. Ed.* **2015,** *54*, 6168-6172; (b) Watabe, T.; Aoki, D.; Otsuka, H. Enhancement of Mechanophore Activation in Mechanochromic Dendrimers by Functionalization of Their Surface. *Macromolecules* **2021,** *54*, 1725-1731; (c) Seshimo, K.; Sakai, H.; Watabe, T.; Aoki, D.; Sugita, H.; Mikami, K.; Mao, Y.; Ishigami, A.; Nishitsuji, S.; Kurose, T.; Ito, H.; Otsuka, H. Segmented Polyurethane Elastomers with Mechanochromic and Self-Strengthening Functions. *Angew. Chem. Int. Ed.* **2021,** *60*, 8406-8409; (d) Ishizuki, K.; Aoki, D.; Goseki, R.; Otsuka, H. Multicolor Mechanochromic Polymer Blends That Can Discriminate between Stretching and Grinding. *ACS Macro Lett.* **2018,** *7*, 556-560.

(19) Hong, G.; Antaris, A. L.; Dai, H. Near-infrared fluorophores for biomedical imaging. *Nat. Biomed. Eng.* **2017,** *1*, 0010.

(20) Ho, C. S. H.; Lim, L. J. H.; Lim, A. Q.; Chan, N. H. C.; Tan, R. S.; Lee, S. H.; Ho, R. C. M. Diagnostic and Predictive Applications of Functional Near-Infrared Spectroscopy for Major Depressive Disorder: A Systematic Review. *Front. Psychiatry* **2020,** *11*, 378.

(21) Yang, G.; Guo, Z.; Bao, Z.; Zhao, J.; Jiang, D.; Yan, L. Review of Anti-counterfeiting of Prints Based on Infrared Spectroscopy. In *Advances in Graphic Communication, Printing and Packaging*, Zhao, P.; Ouyang, Y.; Xu, M.; Yang, L.; Ren, Y., Eds. Springer: Singapore, 2019; Vol. 543, pp 150-156.

(22) Gu, M.; Zhang, Q.; Lamon, S. Nanomaterials for optical data storage. *Nat. Rev. Mater.* **2016,** *1*, 16070.

(23) Wang, S.; Li, B.; Zhang, F. Molecular Fluorophores for Deep-Tissue Bioimaging. *ACS Cent. Sci.* **2020,** *6*, 1302-1316.

(24) Feng, L.; Chen, W.; Ma, X.; Liu, S. H.; Yin, J. Near-infrared heptamethine cyanines (Cy7): from structure, property to application. *Org. Biomol. Chem.* **2020,** *18*, 9385-9397.

(25) (a) Wang, X.; Gu, C.; Zheng, H.; Zhang, Y.-M.; Zhang, S. X.-A. A Multi-Stimuli-Responsive Oxazine Molecular Switch: A Strategy for the Design of Electrochromic Materials. *Chem. Asian J.* **2018,** *13*, 1206-1212; (b) Tomasulo, M.; Sortino, S.; Raymo, F. M. A Fast and Stable Photochromic Switch Based on the Opening and Closing of an Oxazine Ring. *Org. Lett.* **2005,** *7*, 1109-1112.

(26) (a) May, P. A.; Moore, J. S. Polymer mechanochemistry: techniques to generate molecular force via elongational flows. *Chem. Soc. Rev.* **2013,** *42*, 7497-7506; (b) Caruso, M. M.; Davis, D. A.; Shen, Q.; Odom, S. A.; Sottos, N. R.; White, S. R.; Moore, J. S. Mechanically-Induced Chemical Changes in Polymeric Materials. *Chem. Rev.* **2009,** *109*, 5755-5798.

(27) (a) Beyer, M. K. The mechanical strength of a covalent bond calculated by density functional theory. *J. Chem. Phys.* **2000,** *112*, 7307-7312; (b) Klein, I. M.; Husic, C. C.; Kovács, D. P.; Choquette, N. J.; Robb, M. J. Validation of the CoGEF Method as a Predictive Tool for Polymer Mechanochemistry. *J. Am. Chem. Soc.* **2020,** *142*, 16364-16381.

(28) Erbas-Cakmak, S.; Kolemen, S.; Sedgwick, A. C.; Gunnlaugsson, T.; James, T. D.; Yoon, J.; Akkaya, E. U. Molecular logic gates: the past, present and future. *Chem. Soc. Rev.* **2018,** *47*, 2228-2248.

Table of Contents artwork